Available online at www.sciencedirect.com
ScienceDirect
Applied Acoustics 70 (2009) 142–152
applied acoustics
www.elsevier.com/locate/apacoust

Active absorption to reduce the noise transmitted out of an enclosure

Jean-Baptiste Dupont, Marie-Annick Galland *

Centre Acoustique – Laboratoire de Mécanique des Fluides et d'Acoustique, UMR CNRS 5509, École Centrale de Lyon, FR-69134 Écully Cedex, France

Received 11 June 2007; received in revised form 17 December 2007; accepted 17 December 2007
Available online 8 February 2008

Abstract

This paper investigates the potential of active absorbers for reducing low-frequency noise transmission through an enclosure. Active absorbers are intended to obtain a purely real prescribed impedance at the front face of a porous layer. This is achieved by an active control system which cancels the acoustic pressure at the rear face. The test bench was a simplified enclosure: a rigid-wall cavity coupled to a baffled elastic plate. The modeling of the system was based on an analytical modal approach. The purpose of this simulation was first to calculate the optimal impedance, providing maximal reduction in radiated power, and then to define a sub-optimal strategy for actual absorber production. Two 3-cell configurations were implemented on the test bench. Active control used a multichannel feedforward algorithm. In line with prediction, the absorbers provided a 5.5 dB overall reduction while covering only 2% of the cavity surface.

PACS: 43.50.Gf; 43.50.Ki; 43.55.Ev

Keywords: Active noise control; Sound absorber; Acoustic enclosure

1. Introduction

The protection against the excess of noise in the workplace is a crucial public health problem. Machine noise can be controlled by acoustic enclosures which limit the power of outward sound. But this solution often proves to be insufficient, especially for low frequencies. Two main approaches can be envisaged to increase reduction in the noise transmitted by enclosures. The first is wall treatment to absorb acoustic energy inside the enclosure. Lai et al. [1] coated an experimental enclosure by classical passive absorbing materials. Bécot and Sgard [2] investigated the use of poro-elastic and meso-heterogeneous porous materials. For low frequencies, however, these approaches involve an excessive thickness of material. The second approach consists in directly acting on the walls to prevent noise transmission by reducing wall vibration. Generally, covering the walls with passive materials adds mass and increases damping. Sound insulation by double or sandwich panels is also a classical and efficient mean [3,4]. These techniques give good results for high frequencies but reduction remains small at the resonating frequencies of the system.

In consequence, these strategies have to be enhanced to improve low-frequency insulation of enclosures. This was the aim of the CAHPAC project (supported by INRS,[1] CNRS[2] and MENESR[3]). Both of the above approaches are being investigated in particular through active means which ar generally efficient at low frequencies.

Nearby problems were broached in the literature. In particular the inverse problem, i.e., the transmission of the noise through a panel into a cavity was studied for an acoustic excitation outside the enclosure or mechanic excitation on the walls. Pan and Bies [5] detailed the behavior of this type of coupled systems. They also proposed to

* Corresponding author. Tel.: +33 472 18 60 13; fax: +33 472 18 91 43.
E-mail address: marie-annick.galland@ec-lyon.fr (M.-A. Galland).

[1] Institut National de Recherche et de Sécurité.
[2] Centre National de la Recherche Scientifique.
[3] Ministère de l'Éducation Nationale, de l'Enseignement Supérieur et de Recherche.

0003-682X/$ - see front matter © 2007 Elsevier Ltd. All rights reserved.
doi:10.1016/j.apacoust.2007.12.008

reduce the power transmitted into the cavity by controlling the walls' vibration [6–8]. Lacour et al. [9] proposed to use active absorbers inside cavity.

In this study, the problem is different. The objective is to reduce the sound power transmitted by the enclosure's walls toward the outside. Different active strategies can be considered to reduce low-frequency transmission. Active wall vibration control was investigated in many studies. For example, Fuller et al. [10] dealt with different types of actuators and sensors to realize an active structural acoustic control of the sound radiated by a wall. Gardonio et al. [11–13] examined the potential of active panels to control sound transmission. They developed a smart panel prototype with 16 decentralized vibration control units, each consisting of a collocated accelerometer and sensor and piezoceramic patch actuator with a single-channel velocity feedback controller to generate active damping. Moreover, active methods can prevent structures from radiating sound power by providing damping. Adachi et al. [14] sought to develop an active/passive piezoelectric damping system to reduce the dynamic response of a flexible structure.

To control the impedance of a cavity walls allows to modify the inner acoustic behavior as established by Bobrovnitskii [15]. Here, we propose to implement this principle by using active absorbers initially developed for aeronautic applications [16] by the LMFA Center for Acoustics at the École Centrale de Lyon. The basic principle involves an active control system to cancel the acoustic pressure at the rear face of a porous layer, so as to obtain a purely real impedance at the front face, the value of which depends only on the resistivity and thickness of the material. Reactance reduction generally increases absorption, but the objective remains to yield an impedance as close as possible to the optimal impedance: i.e., which produces the greatest reduction in transmitted noise.

An academic configuration was chosen to enable test bench modeling and comparison with measurements. The system studied in this paper consisted of a flexible rectangular plate coupled to a rigid parallelepiped cavity, with a simple support. It was excited by the pressure generated by an acoustic point-source located in a corner of the cavity. The criterion of interest was the sound power transmitted outwards by the plate. This simplified enclosure provided an interesting model to assess the efficiency of various means of reducing radiated noise.

The complete active absorber design and optimization was complex, mainly because of numerous parameters that had to be taken into account. This paper described the procedure for the cavity/plate system.

After a description of the test bench in Sections 2 and 3 concerns system modeling. Coupled cavity/plate systems have been described in many studies [17–19] and, as in most of these, a modal approach by substructures was used here to model the system. More recent numerical methods could also be used. Boundary element methods (BEM) or coupled boundary element/finite element methods (BEM/FEM) [2] seem to predict system behavior more accurately, but only a modal approach is fast enough to implement absorber optimization. The optimal impedance is deduced from the calculation for the whole frequency range of interest.

Section 4 presents the basic principle of active absorbers. Section 5 deals with the selection of a feasible sub-optimal strategy for absorber production. Finally, the experimental results are presented in Section 6, assessing the reduction achieved with active absorbers.

2. System description

The test bench had to be representative of a real enclosure. It also had to be modeled so as to implement an optimization process for the absorber design. Typical industrial enclosures are boxes where to enclose the noise sources. The walls are thin metal sheets, each contributing to noise transmission. The noise comprises broadband spectra with low-frequency components that are difficult to reduce.

The selected geometry enabled modal investigation, so as to highlight the respective effects of structure and cavity on the modal behavior of the system. Fig. 1 describes the geometry of the system, comprising cavity, plate and source. The plate's dimensions were 0.78×0.85 m, and the cavity was 0.60 m high. The walls were made of 3 cm-thick high-density particle panels and could be considered as perfectly rigid in the modeling. For practical reasons, only two configurations were tested for the absorbers' location on the cavity bottom. Indeed, this was the unique wall that could be changed without modifying the bonding between the plate and the cavity.

The flexible plate was made of aluminum AU4G. Its dimensions were 0.78×0.85 m by 2 mm thick. It was inserted in an infinite rigid baffle, and thus assumed to be radiating in a half space. In practice, the cavity was buried in the glass wool of an anechoic chamber. Only the plate, located at the top of the cavity, emerged. A reflective floor was also installed on the absorbing wall of the chamber, acting as a baffle for the plate. A simple support was also assumed around the whole perimeter. On the test bench, the plate-cavity link was required to match two criteria: to approximate the theoretical simple support, while respecting acoustic sealing between the two media (inside and outside the cavity) without leakage. Aglietti and

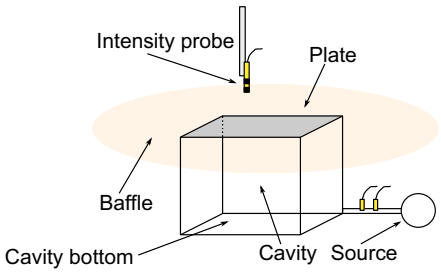

Fig. 1. Scheme of the system.

Cunningham [20] proposed different ways of implementing a simple support condition. Finally, the selected device was inspired by that suggested by Ochs and Snowdon [21]. It was satisfying the two conditions. A 0.2 mm-thick steel strip was stuck (by neoprene) under the plate all along the perimeter, and then gripped by a framework in the upper section of the cavity walls. Thus, on the plate's perimeter, displacement was null. Moreover, as the steel strip was flexible, the plate could rotate locally on the axis of its edge. This provided a simple support. Finally, the steel strip prevented any acoustic outflow. A modal analysis of the uncoupled plate was carried out to check that its behavior was indeed that of a simply supported plate. Table 1 contains the theoretical and experimental frequency values of the first eigen modes of the uncoupled plate. As an indication, the frequencies of the first eigen modes of the rigid cavity are also given. Fig. 2 is an example of the measured modal shapes. Discrepancies between experimental and theoretical eigen frequencies were less than 2%. The experimental modal shapes also corresponded to the theoretical ones. Thus, the plate could be considered as being simply supported.

The source was taken to be a point-source located in the corner of the cavity, at coordinates $(0,0,0)$, emitting in the 50–600 Hz range. On the test bench, a compression driver emerged into a rigid low section tube which arrived in one corner of the cavity. Two microphones located inside the rigid tube measured the sound power injected into the system as well as the acoustic flow of the source.

Lastly, the power transmitted outwards by the plate was measured by an intensimetry probe located at the extremity of a bar which swept the plate surface at a very short distance above it, covering a 132-point grid. Acoustic intensity was then integrated on the whole radiation surface to obtain the power radiated by the plate. The radiated power values were normalized by the sound power injected into the cavity.

Table 1
Theoretical and experimental eigen frequencies (Hz)

Plate				Cavity			
p	q	f_{theo}	f_{exp}	m	n	t	f_{theo}
1	1	14.7	16.3	0	0	0	0
1	2	34.8	35.5	0	1	0	201.8
2	1	38.6	37.8	1	0	0	219.9
2	2	58.7	59.6	0	0	1	285.8
1	3	68.3	69.9	1	1	0	298.4
3	1	78.4	76.9	0	1	1	349.9
2	3	92.2	92.3	1	0	1	360.6
3	2	98.5	98.3	0	2	0	403.5
1	4	115.2	115.0	1	1	1	413.2
3	3	132.0	128.3	2	0	0	439.7
4	1	134.1	131.4	1	2	0	459.5
2	4	139.1	138.9	2	1	0	483.8
4	2	154.2	152.3	0	2	1	494.5
1	5	175.6	172.5	2	0	1	524.5
3	4	178.9	178.2	1	2	1	541.2
4	3	187.7	184.4	2	1	1	562.0
2	5	199.5	196.3	0	0	2	571.7
5	1	205.8	203.1	2	2	0	596.8
5	2	225.9	219.6	0	3	0	605.3
4	4	234.7	231.7	0	1	2	606.2

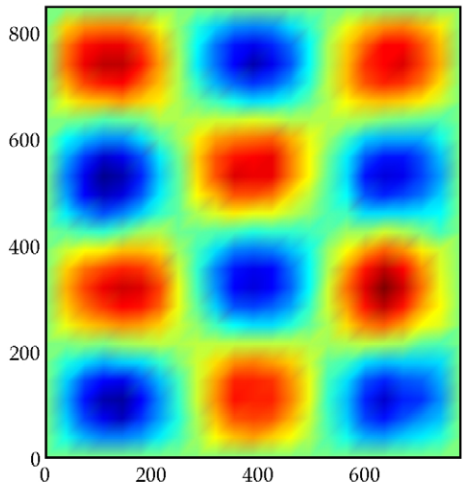

Fig. 2. An example of an experimental modal shape – (3,4) plate mode – $f = 178.2$ Hz.

3. Modeling the system

3.1. A modal approach

The aim of the model was to predict the power transmitted by the plate as a function of the absorbers' situation, size and impedance. The analytical method selected predicted the behavior of the system by expanding the variables on the eigen modes of the rigid cavity and plate. The method was first developed by Lyon [17] and Dowell and Voss [18]. Other studies shed light on sound transmission [19] and integrated impedance boundary condition in the cavity [22].

The calculations are not presented in this paper. Details can be found in reference [23]. It should just be borne in mind that the presence of absorbers on the cavity walls is expressed by Eq. (1) applied to the absorbers' surface, where the complex impedance Z models a locally reacting absorber:

$$\frac{\partial p}{\partial n} = -\mathrm{j}\rho_0\omega\frac{p}{Z} \tag{1}$$

The couplings between the subsystems lead to the matrix formulation (2):

$$(k^2\mathbf{M} - \mathrm{j}k\mathbf{C} - \mathbf{K})(\mathbf{X}) = (\mathbf{F}) \tag{2}$$

where $\mathbf{M}$ is a mass matrix which in particular represents the coupling between the acoustic and structural modes due to the velocity continuity; $\mathbf{C}$ is a damping matrix which represents the acoustic intermodal coupling due to the absorbers in the cavity; $\mathbf{K}$ is a stiffness matrix which also depends on the terms of spatial coupling between the cavity and plate modes; $\mathbf{F}$ is the vector of the modal amplitudes of the excitation; and $\mathbf{X}$ is the vector of the generalized coordinates:

the modal amplitudes of the pressure and displacement. Note that, in the modeling, the system is excited by an acoustic flow source.

System damping was modeled by structural damping. For the first eigen modes of the plate, the modal damping values were adjusted on the modal analysis values. For the higher-order eigen modes, damping was set at 1%.

This modal method enabled the pressure inside the cavity and the velocity field on the plate to be calculated, but neglecting fluid loading outside the cavity. Thus, the radiated sound power was calculated only in terms of the velocity field on the plate. The method selected used the intermodal radiation impedance matrix, the terms of which represent the direct radiation influence of one plate mode on another: they are not really impedances, but represent the radiated pressure effects integrated on the plate surface. According to Lesueur [24], coupling by intermodal radiation is negligible for light fluids (air), and only the real part of the radiation impedance was taken into account. The non-diagonal elements of the matrix were ignored, and only the influence of a mode on itself was considered. Maidanik [25] evaluated the real part of these diagonal terms. Under these assumptions, the radiated power was obtained by a simple matrix product, which reduced computation time considerably. This was necessary in order to implement absorber optimization.

3.2. Typical response of the coupled cavity/plate system

In this section, we consider the case where no active absorber is inserted into the cavity, and the only dissipation is due to the damping of the system (air and plate). The sound power radiated by the plate is examined in Fig. 3. The power radiated is shown as a thin line, the third-octave values as a thick line.

The graph shows the coupled behavior of the system. As stated by Pan and Bies [5] the modes can be cavity-controlled or plate-controlled. A cavity-controlled mode has most of its energy stored in the cavity sound field, while a plate-controlled mode has most of its energy stored as plate vibrational energy.

The first non-zero eigen frequency of the cavity occurres at approximately 200 Hz. Up to this frequency, the modes are plate-controlled and two resonances appear clearly at 69 and 79 Hz. They are associated with the (1,3) and (3,1) plate modes. Note that the first plate mode (1,1), at 33 Hz, is not reproduced in the graph. The plate modes which are anti-symmetric are only weakly excited.

At higher frequencies, the behavior of the system is controlled by the cavity modes. Above 200 Hz, all the cavity-controlled resonances contribute to the radiated sound. Except for the (1,6) plate mode at 250 Hz, they are mainly responsible for the sound radiated from 200 to 600 Hz.

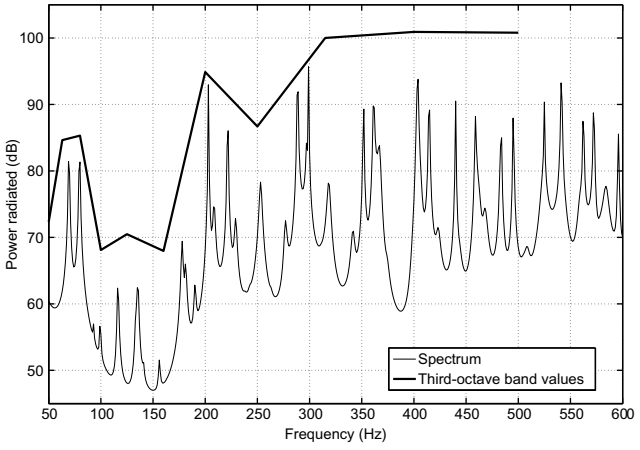

Fig. 3. Sound power radiated by the rigid cavity/plate system – calculation.

4. Basic principle of the active absorber

The basic principle of the active liner has been presented and validated in previous studies [26,16]. It can be summarized as follows: at low frequencies, viscous forces in a porous material predominate over inertial ones and the acoustic behavior is mainly described by the flow resistivity of the material, defined by

$$\sigma = \frac{p_1 - p_2}{ev} \tag{3}$$

where e is the thickness of the porous layer; p_1, p_2 and v represent, respectively, the acoustic pressure and the velocity. If the pressure vanishes at the rear face (i.e., $p_2 = 0$) the layer input impedance $Z = p_1/v$ becomes the flow resistance of the material sample: $Z = \sigma e$. A predetermined purely real impedance can be achieved by selecting a porous material the characteristics of which correspond to the desired condition.

Active control techniques appear to be particularly effective in obtaining the $p_2 = 0$ condition. The secondary source generates a pressure wave, which cancels out the primary one by destructive interference at the microphone location, just behind the porous layer. Hence, broadband excitations can be controlled with a reduced absorbent thickness. Fig. 4 describes the basic principle of the active absorber. This method also offers the advantage of separating the control system from a hostile environment (air flow or hot stream, for instance). In previous projects, different prototypes were developed for flow duct applications [27,28].

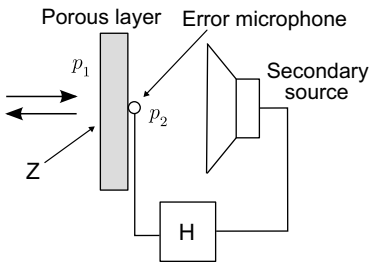

Fig. 4. Basic principle of the active absorber.

For example, this kind of absorber allows to obtain perfectly absorbing walls (Normal incidence absorption coefficient equal to 1) over a wide frequency range in the low frequencies, what is impossible by using a classical passive material or a resonant passive device.

5. Optimization process

5.1. Calculation and measurement of the reduction

The main goal of our study is to obtain the greatest reduction in the sound power transmitted by the plate. Usually, the performances of the acoustic treatments are characterized by their insertion loss factor, which is the reduction in transmitted power obtained thanks to the device compared to the untreated case for a constant injected sound power. This indicator is in conformity with the real industrial machines which deliver a constant sound power. This is why, to analyze the performances of the active absorbers, the measured sound powers must be normalized by the sound power injected into the cavity.

But in the majority of modelings, the noise sources can be only modeled as acoustic volume flow sources. The calculation presented in this paper allows us to determine the power transmitted by the plate as a function of the acoustic volume flow injected into the system. Generally, this distinction is not prejudicial if the reduction device does not modify excessively the radiation impedance of the source as observed in application. In order to reproduce the same conditions in calculation and measurement, it has been decided in this study to present the compared results by using a normalization of the sound powers by the acoustic volume flow injected in the system. This quantity was measured thanks to the two-microphone probe located inside the source's tube.

5.2. Optimal impedance

For each frequency, the radiated power was evaluated according to the calculation described in Section 3, as a function of the complex value of the absorber impedance Z and of the absorbers' situation and size. The optimal impedance was defined as that which, for each frequency, produced the best reduction in the sound power radiated by the plate.

The transverse size of the cell was determined from the bandwidth of interest, and had to ensure a homogeneous pressure field over the cross-section. In our study, the frequency range was 50–600 Hz. Thus, the minimal wavelength was approximately 57 cm, and a 15 cm square cell was selected. Practical considerations concerning the control filter limited the number of active cells in the cavity to 3.

In this paper, two configurations are examined, corresponding to those implemented on the test bench. In configuration A (Fig. 5), 3 cells were laid out side by side on the cavity bottom, in the corner opposite to the source. In configuration B (Fig. 6), 3 cells were placed one in each of 3 corners.

Fig. 7 shows the curve of optimal impedance versus frequency for configuration A. It is normalized by the impedance of air $Z_0 = \rho_0 c_0$. Fig. 8 shows the radiated sound power for the untreated cavity (dotted line) and for the optimal case (solid line) in the case of a source having an acoustic volume flow equal to 1. Third-octave band values are shown as thick lines. The calculated optimal impedance is quite

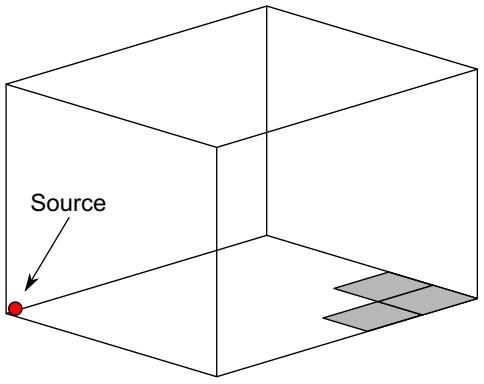

Fig. 5. Configuration A.

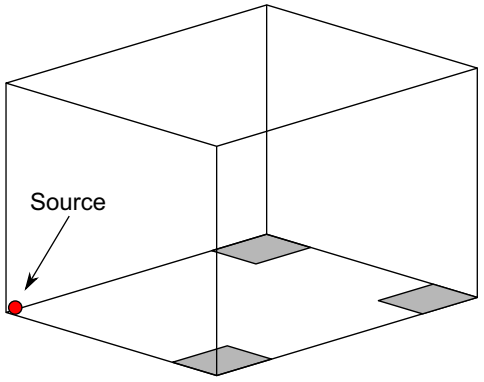

Fig. 6. Configuration B.

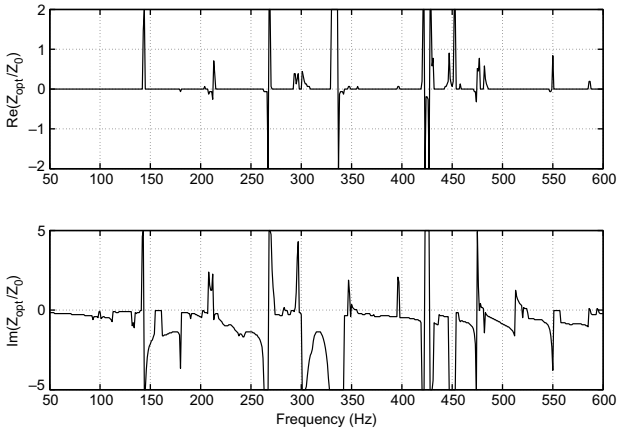

Fig. 7. Optimal impedance (configuration A).

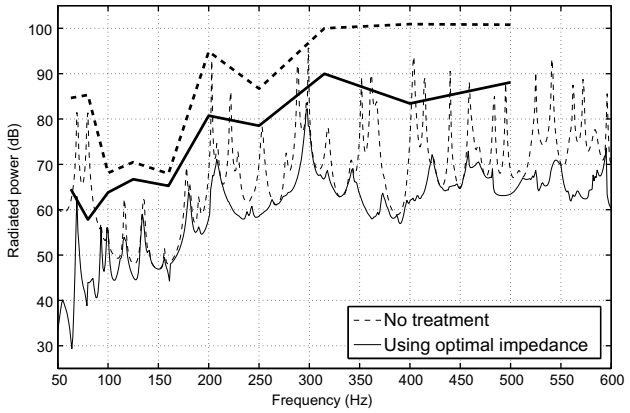

Fig. 8. Radiated power obtained using the optimal impedance (configuration A) – calculation.

purely imaginary: it cannot dissipate energy. The optimal impedance prevents the source from radiating sound. As shown by Nelson et al. [29], the optimal solution is that which minimizes the radiation of all the sources and significantly reduces the noise transmitted by the plate. Moreover, it is effective in both frequency domains (plate-controlled and cavity-controlled). Unfortunately, however, such an impedance was not attainable with our active cells. The value of the imaginary part of Z/Z_0 varied too quickly, whereas it was possible to implement only impedances which were almost independent of frequency [27].

5.3. Sub-optimal impedance

Another strategy was then envisaged, considering cell impedance not to vary with frequency. At each frequency, the impedance was non-optimal, but its value was chosen to reach a compromise. Thus, a sub-optimal strategy was defined by determining the complex impedance which minimized the radiated power level integrated over the whole

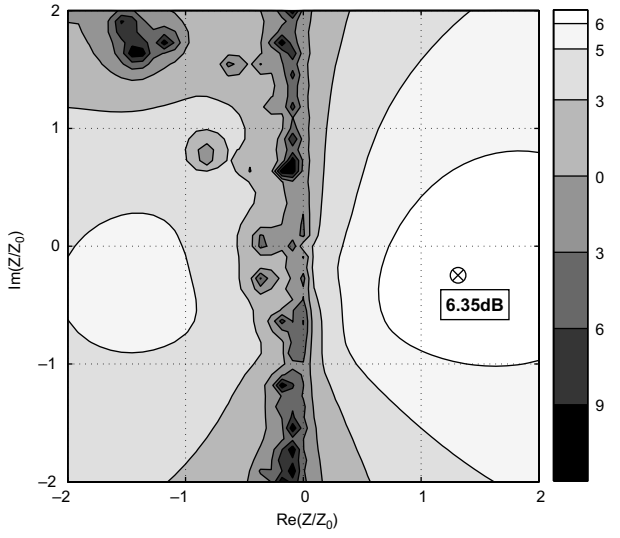

Fig. 9. Noise reduction (dB) as a function of the complex impedance of the absorbers (configuration A).

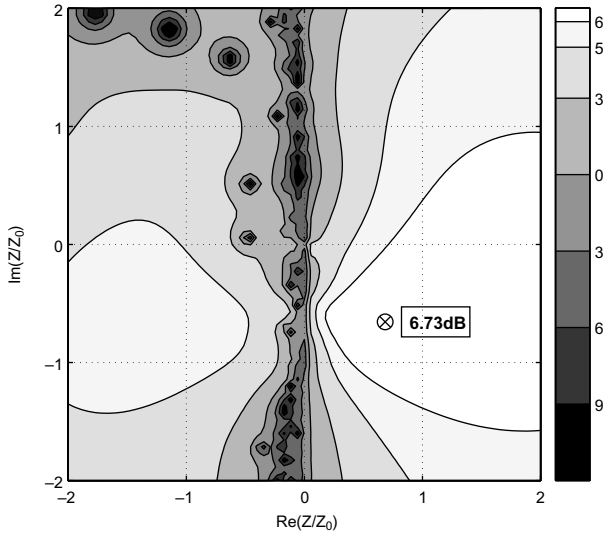

Fig. 10. Noise reduction (dB) as a function of the complex impedance of the absorbers (configuration B).

frequency range. Figs. 9 and 10 show the noise reduction in the transmitted sound power obtained thanks to the active absorbers. It is calculated as a function of the complex impedance of the absorbers for configurations A and B. These figures were obtained by sweeping the impedance complex plan. The sub-optimal impedances obtained are indicated by a cross:

- Configuration A: $Z_{\text{s-opt}}/Z_0 = 1.30 - 0.14\text{i}$
- Configuration B: $Z_{\text{s-opt}}/Z_0 = 0.69 - 0.65\text{i}$

Whereas the optimal impedances are purely imaginary, it can be seen from Figs. 9 and 10 that the sub-optimal impedances had a real part close to 1. In both cases, the reduction was greater than 6 dB over a wide area of the complex plane. These areas included impedance $Z/Z_0 = 1$, and the reduction achieved was hardly any smaller if impedance $Z = Z_0$ was used. Theoretically, the radiated power is reduced by more than 6 dB compared to 12 dB obtained with the optimal impedance. As shown in Fig. 11 and 12, the reductions are significant, in particular for the high frequencies (>200 Hz). At low frequencies, there is no effect. The absorbers perform absorption in the cavity. Fig. 13 shows the reduction in potential acoustic energy of the air cavity with respect to the complex impedance. Although the sub-optimal impedance was not that which gave the best reduction in acoustic potential energy, it was nevertheless close to $Z = Z_0$ and allowed a high degree of acoustic energy absorption. Thus, they allow a reduction of the peaks due to the cavity-controlled modes. But they cannot act on the plate-controlled modes whose energy is stored as plate vibrational energy as evocated in paragraph 3.2.

In the low frequencies (50–200 Hz), the optimal impedance is close to 0. Thus, we can think that by implementing a classical active noise control, we could obtain an interest-

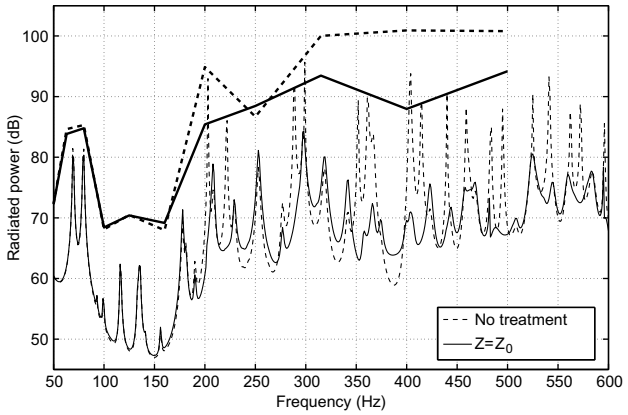

Fig. 11. Power radiated by the plate using Z_0 impedance (configuration A) – calculation.

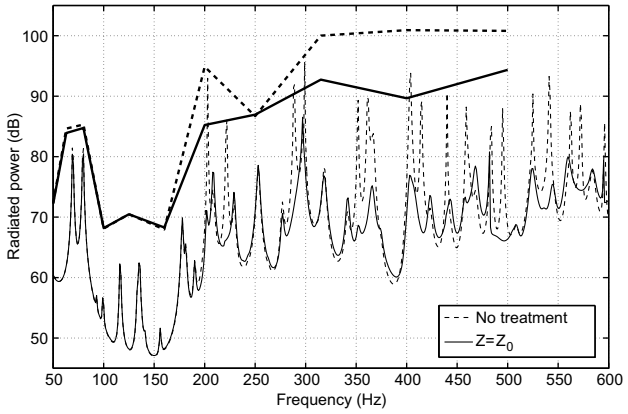

Fig. 12. Power radiated by the plate using Z_0 impedance (configuration B) – calculation.

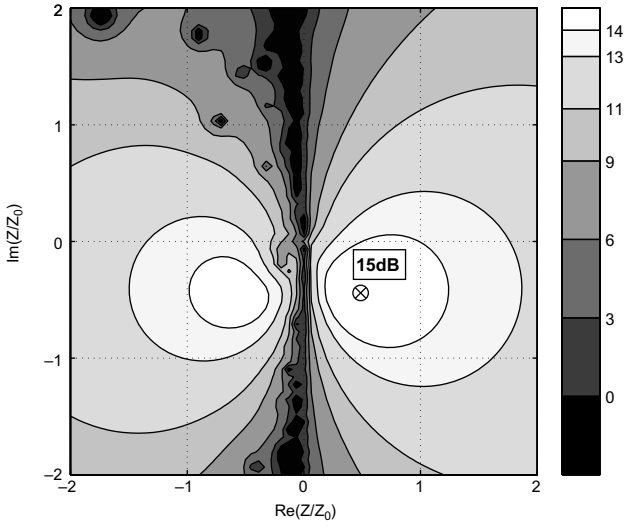

Fig. 13. Reduction (dB) in acoustic potential energy as a function of the complex impedance of the absorbers (configuration A).

ing reduction in this frequency range. However, simulations showed that an impedance equal to zero causes an increase in the sound power transmitted by the plate. A precise realization of the optimal impedance is required (particularly of the reactance) if no absorption occurs. This result is similar to those obtained by Sellen [30] in the case of a treated flow duct.

Other configurations were simulated, while varying the location of the absorbers, for example placing them for example on lateral walls. The results were almost similar. In the same way, wider treatment surfaces were studied. The reduction was all the more important as treated surface was large, but the conclusions remain the same ones: the most efficient transmitted noise reduction strategy consists in absorbing the acoustic energy in the cavity by active absorbers with an impedance close to Z_0.

6. Experimental implementation

6.1. The absorbing cells

An impedance close to Z_0 was obtained by selecting a porous layer such that $\sigma e = Z_0$. Sellen [30] described how to select the material, and characterized series of current materials acoustically. Finally, a wire mesh manufactured by Gantois (Saint Die de Vosges, France), with a resistance very close to Z_0, was selected; this is a high resistance material, so that the porous layer was very thin (less than 1 mm) and the low-frequency behavior of the porous material was confirmed up to 600 Hz. Figs. 14 and 15, respectively, show an assembled cell and three cells inserted in the cavity bottom (configuration B).

6.2. Design of the multiple-channel active control system

Although the aim of active control in this study was to achieve a local control of impedance by reducing the pressure at the rear face of each cell, a MIMO system was required. Indeed, each control microphone received the contribution of all sources (primary and secondary). The electric signal supplying the primary source was a reference signal presenting a high coherence with the noise to be reduced. It also had the great advantage of not being sensitive to the secondary sources, so that there were no

Fig. 14. An assembled cell.

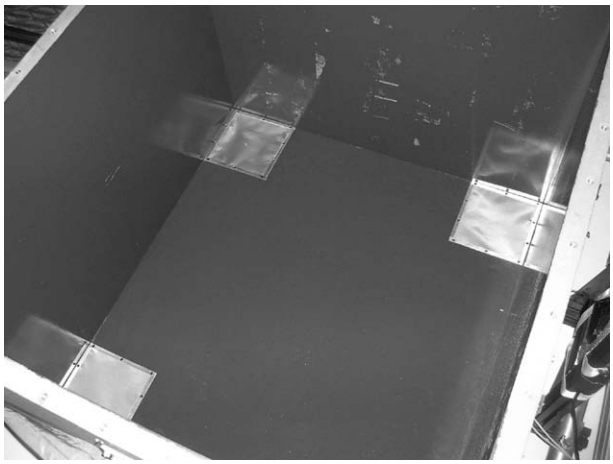

Fig. 15. Three cells inserted in the cavity bottom (configuration B).

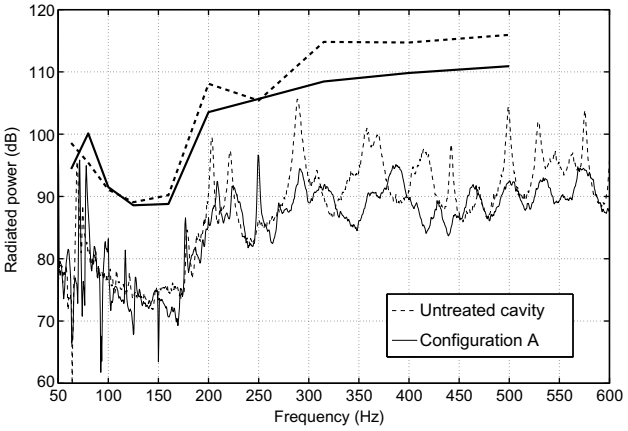

Fig. 16. Experimental results: radiated power (configuration A).

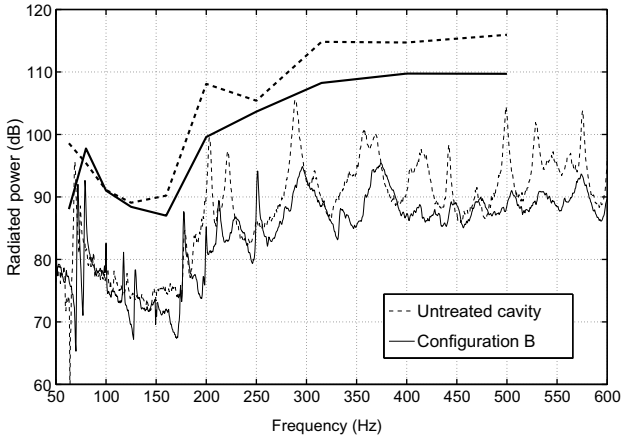

Fig. 17. Experimental results: radiated power (configuration B).

feedback paths from the secondary sources to the reference sensor. The classical FXLMS algorithm was used to reduce noise over the whole frequency range, after a preliminary identification step modeling the secondary paths from the secondary sources to the control microphones.

Nelson and Elliott [31] presented the architecture of the MIMO-FXLMS algorithm, which considers all the secondary paths between the secondary sources and the control microphones. This algorithm was used for the active control implementation.

The control and filtering algorithms were implemented on a dSPACE-DS1103 controller board equipped with a TI-TMS320F240 floating-point DSP. The Simulink controllers were compiled, linked and downloaded to the DSP via the TI-F240 compiler and MATLAB/Real-Time-Workshop. Real-time signal monitoring used the graphic interface of the dSPACE ControlDesk. All acquisitions were made with a Hewlett–Packard data acquisition system piloted by MATLAB.

The primary signal feeding the compression driver was a random noise in the 50–600 Hz frequency range. The DSP board calculated the 155-tap FIR filters of the controllers at a sampling rate of 1.6 kHz. Off-line modeling was first performed to estimate the transfer functions of secondary paths, using 64-tap FIR filters, with an internally-generated white noise driving the secondary source. This identification path included the digital-to-analog (D/A) converter, reconstruction filter (700 Hz), power amplifier, loudspeaker, acoustic path from transducer to error sensor, error sensor, preamplifier, analog-to-digital converter (A/D) and anti-aliasing filter (700 Hz).

6.3. Experimental results

The sound power radiated by the plate was measured by intensimetry. The measured values were normalized for each frequency by the sound power injected into the cavity, the narrow band values of the presented radiated power correspond to an injected power of 1 W/Hz. Figs. 16 and 17 present the results for configurations A and B, showing the sound power radiated by the plate with (solid line) and without (dotted line) the active absorbers; the third-octave band values are shown as thick lines. It has been observed that the sound powers injected into the system measured for each configuration (which are not presented in this paper) are equal. That means that the absorbers did not modify the radiation impedance of the source.

In accordance with calculation, the frequency range could be divided into two parts. Below 200 Hz, radiation was due to the plate-controlled modes, and acoustic absorption did not substantially reduce the transmitted power. Peaks corresponding to the first plate modes (1, 3) and (3, 1), measured at 71 and 78 Hz, were not damped. Moreover, minor peaks were generated between 80 and 150 Hz. Above 200 Hz, all the peaks corresponding to cavity-controlled modes were significantly damped by the active absorbers. On the other hand, because of the absorbers, a peak appeared at 250 Hz. This phenomenon was predicted by calculation (see Fig. 11, for example). The peak matched the (6, 1) plate mode. The absorbers modified the symmetry of the pressure field in the cavity, especially close to the plate. The (6, 1) plate mode was more highly

coupled to the pressure field and thus more highly excited; consequently, at 250 Hz, it radiated more power and the noise transmitted by the plate increased. Finally, configurations A and B reduced the overall level in the experiment by 5.2 and 5.6 dB, respectively, whereas modeling predicted maximum reductions of 6.3 and 6.7 dB. These reductions were mainly achieved in the 200–600 Hz range, controlled by the cavity modes.

The signals measured at the error microphones of the cells assessed the performance of the active control system. Fig. 18 represents an example of the error signal spectrum with (solid line) and without control (dotted line); as previously, the third-octave band values are shown as thick lines. The reduction in overall level with active control was about 20 dB, which validated the active control operation. Reduction varied noticeably over the frequency range, being considerable in the 200–600 Hz range, but definitely lower for the other frequencies. However, since the first cavity mode was approximately located at 200 Hz, the acoustic energy contained in the cavity was much lower below 200 Hz. The FXLMS algorithm was more effective at the frequencies where the energy of the error signal concentrated. Thus, the differences in control performance were quite normal.

The optimal transfer functions of the control filters can be deduced from the measurement of all the secondary and primary paths, and compared to the transfer functions performed after the convergence process. Fig. 19 presents this comparison for one cell. The transfer functions realized very closely approximated the optimal transfer functions. The differences in magnitude were often less than 1 dB. On the bandwidth of interest, the error in phase was also very slight (<2°). This comparison confirmed the good performance of the active control system. However, as noted previously, discrepancies were significant over the 50–200 Hz frequency range, in particular with respect to phase. Active control was not very successful in this range due to the relative weakness of the signal to reduce.

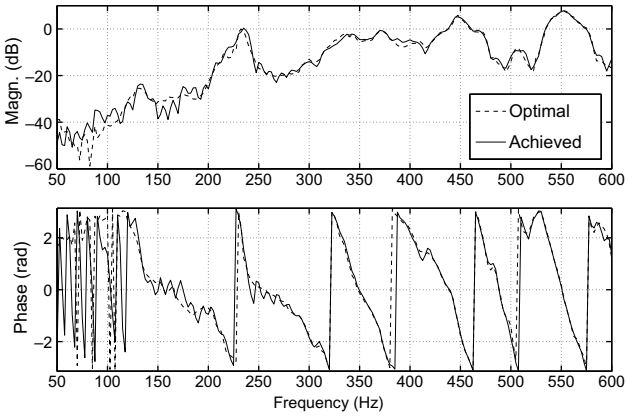

Fig. 19. Comparison between the optimal and achieved transfer function for the controller of one cell.

Thus, in the range 50–200 Hz, the absorbers did not carry out a Z_0 impedance, which was not very penalizing insofar as no reduction was awaited in the theory, even for $Z = Z_0$. Therefore, the results are significant mainly in the range 200–600 Hz.

6.4. Comparison of calculation and measurement

Figs. 20–22 compare calculations and measurements of radiated power in an untreated cavity for configurations A and B. The calculated radiated power is shown as a dotted line and the measurement as a solid line. As noted in the Section 5.1, to be compared to the calculated radiated powers, the measured powers were normalized by the injected acoustic flow. In each case, the calculated radiated power was adjusted so as to obtain the same overall power level as the measured one.

For the rigid cavity, results were in good agreement: third-octave band values were similar, and the same phenomena could be found in both measurements and calculations. Below 200 Hz, radiated power was lower. Peaks

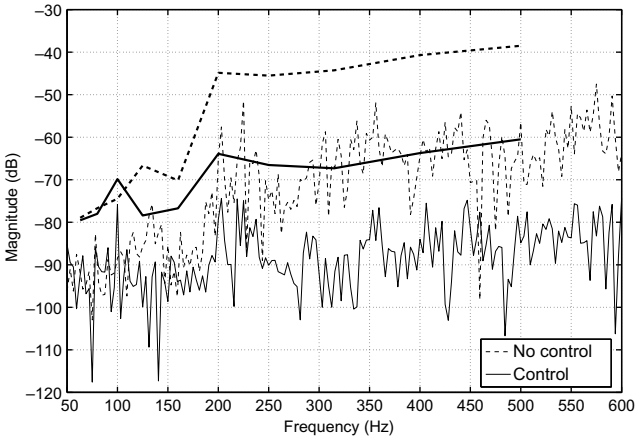

Fig. 18. An example of error signal spectrum.

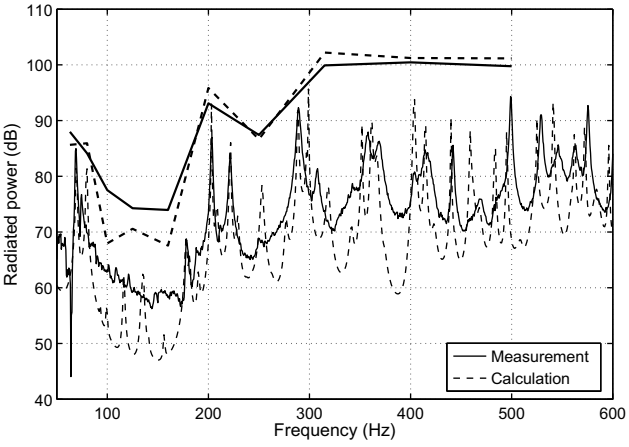

Fig. 20. Comparison of calculation and measurement – untreated cavity.

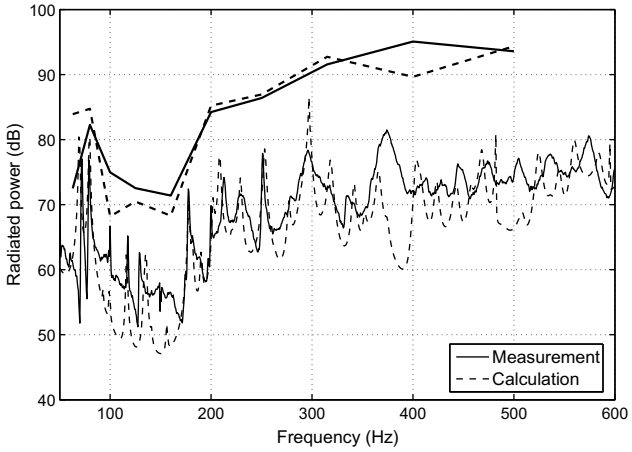

Fig. 21. Comparison of calculation and measurement – configuration A.

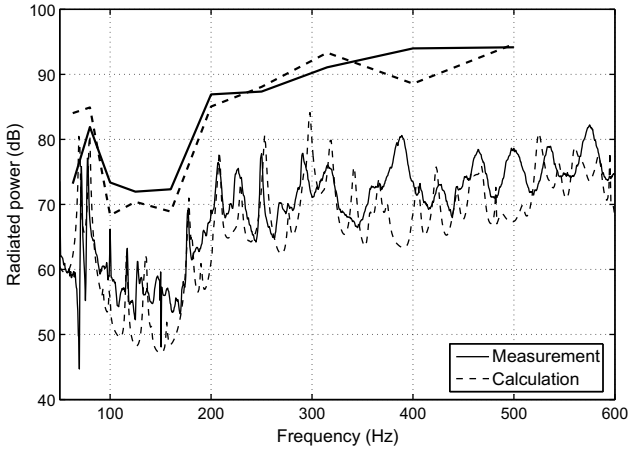

Fig. 22. Comparison of calculation and measurement – configuration B.

corresponding to plate modes (1, 3) and (3, 1) appeared significantly. Above 200 Hz, the peaks corresponded to cavity modes. Calculation predicted peak frequencies very accurately, and predicted relative levels between peaks fairly well. On the other hand, some dissimilarities remained between the curves. The minimum between 80 and 200 Hz was more marked in the calculations than in the measurements. Over the 200–600 Hz range, peaks were more damped in measurements. Moreover, some peaks corresponding to cavity modes barely appeared in the measurements whereas they were quite visible in the calculations. Lastly, in the calculations, some minor peaks revealed an influence of the plate modes above 200 Hz, difficult to discern from the measurements.

The same holds for configurations A and B (Figs. 21 and 22), except that the prediction of the cavity peaks was worse, in particular for high frequencies. For example, for both configurations, measurement presented a maximum around 375 Hz which was not predicted by calculation.

Radiated power was estimated from the radiation impedance matrix. This method is much faster but less accurate than other ones such as boundary element methods. It tends to over-estimate the influence of the plate modes and underestimate that of the cavity modes. This may explain some discrepancies. Moreover, the comparisons showed damping to be underestimated: the structural damping introduced into the analytical calculation did not model the behavior of the system correctly. On the test bench, in addition to the damping of the plate, the steel sheet added a damping which was difficult to consider in the model. The discrepancies observed for configurations A and B can also be explained by two factors: the impedance really achieved may have differed from Z_0, and may not have been uniform over the entire cell surface.

7. Conclusion

This paper investigated the potential of active absorbers for reducing the noise transmitted by an enclosure. A cavity/plate system was studied in the 50–600 Hz frequency range. The most efficient active absorber was designed by modeling the coupled system. The basic principle of the active absorber uses an active control system to obtain a purely real prescribed impedance at the front face of a porous layer. The optimal impedance, defined as that which produces the best reduction in transmitted noise, was calculated for each frequency. Unfortunately, this impedance did not lead to a feasible absorber. Thus, it was necessary to consider another strategy. The sub-optimal impedance was that which gave the best reduction in overall power level over the whole frequency range. Calculation showed it to approximate Z_0, the characteristic impedance of air.

Two 3-cell configurations were implemented on the test bench and active control was performed using a feedforward MIMO controller. In the experiment, reductions greater than 5 dB were obtained with absorbers covering only 2% of the cavity surface. The reduction was especially high on the peaks of the cavity-controlled range (200–600 Hz). The absorbing cells had no effect at low frequencies because the behavior of the system was controlled by the plate modes.

Further experiments will be carried out in order to measure the impedance really achieved by the active absorbers. This experiment should also determine the area on which this impedance is effective. Other control strategies will be studied to enhance the efficiency of active absorbers. For instance, noise reduction would extend to the low-frequency range 50–200 Hz if cell impedance were closer to the optimal impedance. A two-microphone probe could be used to perform a complete control of both reactance and resistance. Over the 200–600 Hz range, the sub-optimal strategy presented in this paper is well suited.

Acknowledgements

This work was supported by INRS (Institut National de Recherche et de Sécurité) and CNRS (Centre National de la Recherche Scientifique) as part of the CAHPAC project.

References

[1] Lai JCS, Speakman C, Williamson HM. Control of shear cutting noise – effectiveness of enclosures. Appl Acoust 1999;58(1):69–84.

[2] Bécot F-X, Sgard F. On the use of poroelastic materials for the control of the sound radiated by a cavity backed plate. J Acoust Soc Am 2006;120(4):2055–66.

[3] Mulholland KA, Parbrook HD, Cummings A. The transmission loss of double panels. J Sound Vib 1967;6(3):324–34.

[4] Tang WC, Zheng H, Ng CF. Low frequency sound transmission through close-fitting finite sandwich panels. Appl Acoust 1998;55(1):13–30.

[5] Pan J, Bies DA. The effect of fluid-structural coupling on sound waves in an enclosure – theoretical part. J Acoust Soc Am 1990;87(2):691–707.

[6] Pan J, Bies DA. Active control of noise transmission through a panel into a cavity: I. Analytical study. J Acoust Soc Am 1990;87(5):2098–108.

[7] Pan J, Bies DA. Active control of noise transmission through a panel into a cavity: II. Experimental study. J Acoust Soc Am 1991;90(3):1488–92.

[8] Pan J, Bies DA. Active control of noise transmission through a panel into a cavity: III. Effect of the actuator location. J Acoust Soc Am 1991;90(3):1493–501.

[9] Lacour O, Galland MA, Thenail D. Preliminary experiments on noise reduction in cavities using active impedance changes. J Sound Vib 2000;230(1):69–99.

[10] Fuller CR, Rogers CA, Robertshaw HH. Control of sound radiation with active/adaptive structures. J Sound Vib 1992;157(1):19–39.

[11] Gardonio P, Bianchi E, Elliott SJ. Smart panel with multiple decentralized units for the control of sound transmission. Part I: theoretical predictions. J Sound Vib 2004;274(1):163–92.

[12] Gardonio P, Bianchi E, Elliott SJ. Smart panel with multiple decentralized units for the control of sound transmission. Part II: design of the decentralized control units. J Sound Vib 2004;274 (1–2):193–213.

[13] Bianchi E, Gardonio P, Elliott SJ. Smart panel with multiple decentralized units for the control of sound transmission. Part III: control system implementation. J Sound Vib 2004;274(1–2):215–32.

[14] Adachi K, Kitamura Y, Iwatsubo T. Integrated design of piezoelectric damping system for flexible structure. Appl Acoust 2004;65(3):293–310.

[15] Bobrovnitskii YI. Active control of sound in a room: method of global impedance matching. Acoust Phys 2003;49(6):620–6.

[16] Galland MA, Mazeaud B, Sellen N. Hybrid passive/active absorbers for flow ducts. Appl Acoust 2005;66(6):691–708.

[17] Lyon RH. Noise reduction of rectangular enclosures with one flexible wall. J Acoust Soc Am 1963;35(11):1791–7.

[18] Dowell EH, Voss HM. The effect of a cavity on panel vibration. AIAA J 1963;1(2):476–7.

[19] Pretlove AJ. Forced vibrations of a rectangular panel backed by a closed rectangular cavity. J Sound Vib 1966;3(3):252–61.

[20] Aglietti GS, Cunningham PR. Is a simple support really that simple? J Sound Vib 2002;257(2):321–35.

[21] Ochs JB, Snowdon JC. Transmissibility across simply supported thin plates. I. Rectangular and square plates with and without damping layers. J Acoust Soc Am 1975;58(4):832–40.

[22] Dowell EH, Gorman GF, Smith DA. Acoustoelasticity: General theory, acoustic natural modes and forced response to sinusoidal excitation, including comparisons with experiment. J Sound Vib 1977;52(4):519–42.

[23] Dupont J-B, Galland M-A, Hybrid absorption to reduce the noise transmitted by a plate coupled to a cavity: determination of the optimal impedance. In: First symposium on the acoustics of poro-elastic materials, E.N.T.P.E, Vaulx-en-Velin, France, December 2005.

[24] Lesueur C. Rayonnement acoustique des structures. Paris: Editions Eyrolles; 1988.

[25] Maidanik G. Response of ribbed panel to reverberant acoustic field. J Acoust Soc Am 1962;34(6):809–26.

[26] Furstoss M, Thenail D, Galland MA. Surface impedance control for sound absorption: direct and hybrid passive/active strategies. J Sound Vib 1997;203(2):219–36.

[27] Galland MA, Mazeaud B, Sellen N. Performance in wind tunnel of hybrid active/passive absorbent panels. In: 10th AIAA/CEAS aero-acoustics conference, Manchester, United-Kingdom. AIAA Paper 2004-2852, 10–12 May 2004.

[28] Mazeaud B, Galland MA, Sellen N. Design of an adaptive hybrid liner for flow duct applications. In: 10th AIAA/CEAS aeroacoustics conference, Manchester, United-Kingdom. AIAA Paper 2004-2852, 10–12 May 2004.

[29] Nelson PA, Curtis ARD, Elliott SJ, Bullmore AJ. The minimum output power of free field point sources and active control of sound. J Sound Vib 1987;117(1):1–13.

[30] Sellen N, Cuesta M, Galland MA. Noise reduction in a flow duct: implementation of a hybrid passive/active solution. J Sound Vib 2006(3-5):492–511.

[31] Nelson PA, Elliott SJ. Active control of sound. New-York: Academic Press; 1991.